

Statistical Model of Optical Coherence Tomography Angiography Parameters That Correlate With Severity of Diabetic Retinopathy

Mohammed Ashraf,^{1,2} Peter L. Nesper,¹ Lee M. Jampol,¹ Fei Yu,³ and Amani A. Fawzi¹

¹Department of Ophthalmology, Feinberg School of Medicine, Northwestern University, Chicago, Illinois, United States

²Department of Ophthalmology, Alexandria Faculty of Medicine, Alexandria, Egypt

³Department of Biostatistics, Fielding School of Public Health, University of California-Los Angeles, Los Angeles, California, United States

Correspondence: Amani Fawzi, Department of Ophthalmology, Feinberg School of Medicine, Northwestern University, 645 N. Michigan Avenue, Suite 440, Chicago, IL 60611, USA; afawzim@gmail.com.

MA and PLN contributed equally to the work presented here and should therefore be regarded as equivalent authors.

Submitted: February 21, 2018

Accepted: July 26, 2018

Citation: Ashraf M, Nesper PL, Jampol LM, Yu F, Fawzi AA. Statistical model of optical coherence tomography angiography parameters that correlate with severity of diabetic retinopathy. *Invest Ophthalmol Vis Sci*. 2018;59:4292-4298. <https://doi.org/10.1167/iovs.18-24142>

PURPOSE. To determine whether combining quantitative optical coherence tomography angiography (OCTA) parameters can achieve high sensitivity and specificity to distinguish eyes with nonproliferative diabetic retinopathy (NPDR) from those with proliferative diabetic retinopathy (PDR) as well as eyes with diabetes and no DR (NoDR) from those with clinical DR (any DR).

METHODS. This cross-sectional study included 28 eyes (17 patients) with NoDR, 54 eyes (34 patients) with NPDR, and 56 eyes (36 patients) with PDR. OCTA images were processed to quantify the foveal avascular zone (FAZ) area, acircularity, vessel density, skeletonized vessel density, fractal dimension, and intersections and average vessel diameter for the superficial (SCP) and the deep capillary plexus (DCP). Binary logistic regression models were used to identify the OCTA parameters that best distinguished DR severity groups. The area (AUC) under the receiver operating characteristic (ROC) curves, and sensitivity and specificity were calculated for each model.

RESULTS. The regression model identified the SCP FAZ area, DCP vessel density, and acircularity as parameters that best distinguished between DR severity groups. ROC curves for NPDR versus PDR had an AUC of 0.845 ($P < 0.001$) and sensitivity and specificity of 86% and 70%, respectively. ROC curves for NoDR versus any DR showed an AUC of 0.946 ($P < 0.001$) with sensitivity of 89% and specificity of 96%, with comparable results when explored in males and females separately.

CONCLUSIONS. We identified a set of OCTA parameters with high sensitivity and specificity for distinguishing between groups based on DR severity, suggesting potential clinical application for OCTA as a screening tool for DR.

Keywords: optical coherence tomography angiography, diabetic retinopathy, OCT, retina

Optical coherence tomography angiography (OCTA) is a new, noninvasive modality that visualizes retinal capillary blood flow without the need for intravenous dye.¹ In contrast to fluorescein angiography, OCTA uniquely visualizes individual retinal capillary plexuses, including the superficial capillary plexus (SCP), deep capillary plexus (DCP), and more recently, the middle capillary plexus (MCP).²

Several studies have explored the relationship between individual OCTA parameters and the stage of diabetic retinopathy (DR).³⁻⁹ Of these studies, some have looked at the SCP and DCP separately,^{4,9,10} while others have examined the full-thickness slab of the retina.^{6,7} These studies explored a variety of OCTA parameters, including vessel density,⁹⁻¹¹ skeletonized vessel density,^{9,10} vessel tortuosity,¹² fractal dimensions,^{4,13} adjusted flow index,¹¹ foveal avascular zone (FAZ) parameters,^{8,14-16} and intercapillary spaces.⁶ However, discrepancies exist as to which parameter and/or vascular layer is most representative of changes across DR severity levels. Bhanushali et al.,⁵ using fractal analysis, explored the spacing between vessels and found that parameters in the SCP (not the DCP)

were significantly different between grades of DR. In contrast, Samara et al.⁹ used different parameters (vessel density and skeletonized vessel density) and found that the DCP showed a statistically significant difference between eyes with any stage of nonproliferative DR (NPDR) compared to those with proliferative DR (PDR). Furthermore, using full-thickness slabs, Salz et al.⁷ showed that the perifoveal intercapillary area was significantly different when comparing healthy controls to eyes with any stage of DR, and these same parameters also showed significant differences when comparing eyes with PDR to those with NPDR.

While OCTA parameters have been studied individually, only one study has attempted to combine these parameters to differentiate eyes with and without DR.¹⁷ Furthermore, no study has examined whether combining OCTA parameters can differentiate eyes with NPDR from those with PDR. Therefore, the aim of the present study was to narrow down the complex array of previously studied parameters to a feasible set of parameters that, combined, could differentiate eyes with NoDR from those with any DR as well as differentiate eyes with NPDR

from those with PDR. The overall goal was to identify a minimal set of OCTA parameters that would have high impact in a clinical setting.

METHODS

This was a cross-sectional analysis of a consecutive series of subjects with diabetes who underwent OCTA in the Department of Ophthalmology at Northwestern University in Chicago, Illinois, between June 2015 and December 2016. The study was approved by the Institutional Review Board of Northwestern University, followed the tenets of the Declaration of Helsinki, and was performed in accordance with Health Insurance Portability and Accountability Act regulations. Written informed consent was obtained from all participants.

Study Sample

Inclusion criteria included eyes from subjects with diabetes and no DR (NoDR), eyes with NPDR, and eyes with PDR based on clinical assessment by two experienced, board-certified retina specialists (AAF and LMJ) using the proposed international diabetic retinopathy severity scale.^{18,19} Only eyes that had OCTA images without significant movement or shadow artifacts and with a signal strength index score greater than 50 were considered eligible. Specifically, OCTA images with large motion artifacts that appreciably distorted the retinal vessels (i.e., lateral displacement, vascular doubling, stretch artifacts) or images with areas of attenuation of both the OCTA and OCT signal (i.e., shadowing) were excluded from the analysis. We also did not include eyes with segmentation errors. Exclusion criteria included eyes with other retinal or ocular diseases that may confound our results, such as glaucoma. In addition, cases with large macular retinal hemorrhages, high refractive error (more than 6 diopters), or cataract, graded above nuclear opalescence grade three or nuclear color grade three, were excluded in order to avoid optical artifacts that may potentially compromise OCTA image quality.

Image Acquisition

We used the RTVue-XR Avanti OCTA system (Optovue, Inc., Fremont, CA, USA) with split-spectrum amplitude-decorrelation angiography (SSADA) software.¹ This instrument has an A-scan rate of 70,000 scans per second and uses a light source centered on 840 nm and a full-width at half-maximum (FWHM) bandwidth of 45 nm. A 3×3 -mm² scanning area, centered on the fovea, was obtained. Two consecutive B-scans (M-B frames), each containing 304 A-scans, were captured at each sampling location, and SSADA was used to extract OCTA information. En face OCT angiograms were segmented to define the SCP and DCP using the automatic segmentation algorithm of the device (AngioVue software version 2016.1.0.26). The built-in algorithm segments the SCP slab from 3 μ m posterior to internal limiting membrane (ILM) to 15 μ m posterior to the inner plexiform layer (IPL). The DCP slab was segmented from 15 to 70 μ m posterior to the IPL. We relied on automatic segmentation with no attempts at manual alteration of the slabs. Eyes were classified as having diabetic macular edema (DME) if they had both intraretinal cystoid spaces and a central macular thickness (CMT) equal to or greater than 300 μ m. This corresponds to a normal CMT + two standard deviations: $255.2 + (2 \times 22)$ μ m, based on the RTVue normative database of 644 eyes of 364 subjects, as listed in the user manual.

Image Processing

We exported the SCP and DCP angiograms into ImageJ (developed by Wayne Rasband, National Institutes of Health, Bethesda, MD, USA; available in the public domain at <http://rsb.info.nih.gov/ij/index.html>).²⁰ The scale of each 304×304 -pixel en face angiogram was set to 3×3 mm² in ImageJ to conduct the following measurements:

FAZ Area. The FAZ area was measured in each layer (SCP and DCP) separately by a trained retina fellow (MA). Manual tracing of the FAZ was done using the “free hand selection” tool of ImageJ. We utilized the reciprocal ($1 / \text{FAZ area}$) in the regression formula so that correlations for the reciprocal FAZ and other OCTA variables were in the same direction. Previous studies have demonstrated the repeatability and reproducibility of manual tracing of the FAZ.^{3,21}

Acircularity Index. Acircularity represents the degree to which the FAZ is different from a perfect circle, with the value of 1.0 representing a perfect circle.²² We used the manually traced outline of the FAZ in the SCP to perform the acircularity measurement, which can be automatically calculated using the “shape descriptors” option in ImageJ. Previous studies have demonstrated the repeatability of measurements of the FAZ in the SCP as well as the acircularity index.^{3,14} The equation to calculate acircularity in ImageJ was as follows:

$$\text{Acircularity} = \frac{\text{Perimeter of the FAZ}}{\text{Perimeter of the Circle With Equal Area}} \quad (1)$$

Vessel Density (%). We used the built-in AngioVue Analytics software (version 2016.1.0.26) to obtain parafoveal blood vessel density for the SCP and DCP. The “parafovea” was defined as an annulus centered on the fovea with inner and outer ring diameters of 1 and 3 mm, respectively. Vessel density was reported as the percentage of the total area within the parafovea that was occupied by blood vessels. To calculate vessel density, the AngioVue Analytics software extracts a binary image of the blood vessels from the grayscale OCTA image, and then calculates the percentage of pixels occupied by blood vessels in the defined region.

Skeletonized Vessel Density. We used ImageJ software to binarize and skeletonize the vessels into 1-pixel-wide vessels to measure skeletonized vessel length. We used a previously validated binarization technique, which involved duplicating the image and then using a Hessian filter on one and a local median threshold on the other.^{10,23} Only pixels that were common to both images were incorporated in the final analysis. We then divided the skeletonized vessel length by the total retinal area (not including the FAZ) in order to generate the skeletonized vessel density.

$$\begin{aligned} \text{Skeletonized Vessel Density mm}^{-1} \\ = \frac{\text{Total Length of Skeletonized Vessels mm}}{(\text{Total Area} - \text{Area of FAZ})\text{mm}^2} \end{aligned} \quad (2)$$

Fractal Dimension. Fractal dimension quantifies the degree of complexity of an object. The value of the fractal dimension is usually between 1 and 2 when measuring objects in two dimensions, with a higher number indicating greater complexity. The method of fractal analysis has previously been described.⁴ In brief, we used the box counting method in Fractalyse software (ThéMA, Besancon, France) resulting in a fractal dimension value for each image.

Intersections and Average Vessel Diameters. We calculated these parameters using DiameterJ, an open source plugin created for ImageJ developed at the National Institute of Standards and Technology.²⁴ DiameterJ is a validated tool used to measure the diameter of microfibers at every pixel along a fibers axis and produces a histogram of these diameters. It also

provides other data including intersections, which represents the number of points where blood vessels overlap and is calculated using the formula shown in Equation 3.

$$\text{Intersection Density}(\text{100} \times \text{100 pixels}) = \frac{(\text{Number of Fiber Overlaps}) \times \text{10000}}{(\text{Total Pixels in Image})} \quad (3)$$

Statistics

Statistical analysis was performed using a commercially available statistical software program (SPSS for Windows, version 23; IBM/SPSS, Chicago, IL, USA). One-way ANOVA was used to study each OCTA variable across the three DR severity groups (NoDR, NPDR, and PDR). Bonferroni post hoc analysis was conducted to examine the statistically significant differences. Variables that were statistically significant in the univariate analysis were included in a multivariable binary logistic regression model comparing eyes with NPDR versus PDR, using backward elimination for stepwise elimination of the nonsignificant variables from the final model. The same model was used to compare eyes with NoDR to eyes with any DR (NPDR and PDR combined). Generalized estimating equation (GEE) was used to correct for the correlation between the two eyes. We also corrected for age and sex. The receiver operating characteristic (ROC) curves were generated based on the binary logistic regression models, and summary statistics, including area under the curve (AUC), sensitivity, and specificity were calculated from the ROC curve. A value of $P < 0.05$ was considered statistically significant.

RESULTS

This study included 28 eyes (17 patients) with NoDR, 54 eyes (34 patients) with NPDR, and 56 eyes (36 patients) with PDR. We found no significant difference between groups with regard to age, type of diabetes (1 or 2), the presence of hypertension, or glycated hemoglobin (Table 1). Eyes with NPDR included 20 eyes with mild NPDR, 26 with moderate NPDR, and 8 with severe NPDR. DME was present in 13 eyes (24%) in the NPDR group, compared to 6 eyes (11%) in the PDR group, all of which had received at least one prior anti-VEGF injection at the time of imaging. None of the eyes with DME had CMT of greater than 385 μm or any appreciable segmentation errors. Thirty-two eyes (57%) in the PDR group had panretinal photocoagulation (PRP) prior to OCTA imaging. No eyes with severe NPDR had received PRP.

Univariate Analysis

Univariate analysis of the individual OCTA parameters identified skeletonized vessel density (SCP), fractal dimension (SCP and DCP), vessel density (SCP and DCP), and acircularity index as significantly different between the DR severity groups. The FAZ (SCP or DCP) was significantly different only when comparing eyes with PDR to either of the two less severe stages. The skeletonized vessel density (DCP) was significantly different when comparing eyes with any stage of DR (NPDR and PDR) to those with NoDR. Other OCTA parameters and comparisons are detailed in Table 1.

Binary Logistic Regression Model

When comparing eyes with NPDR ($n = 34$) to those with PDR ($n = 36$), we used a multivariable binary regression model with backward elimination that included all the variables with statistical significance in the univariate analysis. The regression

model identified the reciprocal FAZ area (SCP), vessel density (DCP), and acircularity index as significant. GEE was used to correct for the correlation between eyes of the same participant (Table 2). We then generated ROC curves for these variables using the combined parameter model (Figure). The AUC for the combined regression model was 0.845 ($P < 0.001$) with sensitivity and specificity of 86% and 70%, respectively. Using the same OCTA parameters, we examined the ROC curves for males and females separately (Figure), and found comparable results although with a slightly higher specificity for females. As shown in Table 3, individually, the OCTA parameters showed lower discrimination values compared to the combined model.

We used the same approach and parameters to evaluate the algorithm in eyes with NoDR ($n = 17$) compared to those with any DR (combined NPDR and PDR; $n = 70$) (Table 4). The ROC curve showed an AUC of 0.946 ($P < 0.001$) with sensitivity and specificity of 89% and 96%, respectively (Table 3; Figure). The model worked equally well in males and females (Table 4).

DISCUSSION

The current study demonstrates that combining a small set of select OCTA parameters improves the overall diagnostic efficacy for discriminating eyes with NPDR from those with PDR (Table 2). Furthermore, the same model accurately distinguished eyes with NoDR from those with any DR (Table 3). From a total of 13 potential OCTA variables, logistic regression with backward elimination identified a combination of three variables that were significant: reciprocal FAZ area (SCP), vessel density (DCP), and acircularity index (FAZ in SCP). The relatively low sensitivity/specificity of the individual parameters compared to the overall combined model highlights the importance of using a combination of variables, which is an important milestone (Table 3). Many parameters such as fractal dimensions and vascularized vessel density previously shown to be of significance did not achieve significance in the final model.^{4,5,9,10,13,15,25,26} In addition, many variables that were significant in the univariate analysis of the current study were not useful in the final model. This could suggest a dichotomy between absolute differences and clinical applicability, and the need for future research to focus on identifying the most clinically relevant parameters, rather than continuing to expand the pool of complex OCTA parameters.

Of the combined parameters, the FAZ (SCP) has been shown to be significantly larger in eyes with DR compared to healthy controls although it had low diagnostic value on its own (AUC 0.472).^{5,9,15,27} In the setting of DR, the FAZ results are highly variable, with some studies finding no differences between NPDR and PDR groups⁹ while others report a significantly larger FAZ (SCP) in eyes with PDR.¹² Our data showed that the FAZ SCP was significantly greater in eyes with PDR compared to eyes with NPDR ($P < 0.001$) (Table 1). In the current study, we used the automated segmentation for SCP with the lower boundary set at 15 μm below to the IPL. Therefore, the SCP actually included the anatomic MCP using this software (version 2016.1.0.26).² The MCP contains the smallest diameter of the FAZ, which could explain why the FAZ area and acircularity in the "SCP" was able to discriminate the stages of retinopathy in our study.

The second parameter, vessel density (DCP), has been previously shown to be significantly different between eyes with mild/moderate NPDR (and not severe) compared with eyes with PDR.^{9,10} Only 15% of eyes in the current study had severe NPDR, which may explain why this parameter was particularly significant at differentiating eyes with NPDR and

TABLE 1. Demographic Characteristics and Univariate Analysis of Individual Optical Coherence Tomography Angiography Parameters

Characteristics	NoDR	NPDR	PDR	NoDR vs. NPDR, <i>P</i> Value*	NoDR vs. PDR, <i>P</i> Value*	NPDR vs. PDR, <i>P</i> Value*
Sex, male:female	6:11	16:18	22:14			
DM type, type 1:type 2	6:11	6:28	12:24	0.168	0.891	0.137
Age	53.66 ± 12.98	53.47 ± 9.46	49.90 ± 14.47	1.00	0.576	0.399
Duration of DM	14.18 ± 16.18	17.76 ± 12.36	22.63 ± 10.30	0.387	0.030*	0.089
HbA1c	7.75 ± 1.68	10.45 ± 10.45	8.47 ± 2.20	0.330	0.277	0.323
Hypertension (%)	10 of 17 (58.8)	18 of 34 (52.9)	27 of 36 (75.0)	0.698	0.239	0.055
Lens, clear:cataract:IOL	12:16:0	22:25:7	21:24:11			
Pars plana vitrectomy	None	None	3 eyes			
Signal strength index	67.11 ± 8.53	66.04 ± 6.66	64.23 ± 8.13	0.533	0.137	0.207
FAZ SCP, mm ²	0.33 ± 0.14	0.33 ± 0.15	0.48 ± 0.23	1.00	0.002*	<0.001*
FAZ DCP, mm ²	0.37 ± 0.14	0.46 ± 0.21	0.65 ± 0.31	0.428	<0.001*	<0.001*
Skeletonized vessel density SCP, mm ⁻¹	13.67 ± 1.71	11.88 ± 2.45	10.87 ± 1.71	0.001*	<0.001*	0.027*
Skeletonized vessel density DCP, mm ⁻¹	16.16 ± 1.46	12.70 ± 3.04	12.32 ± 2.10	<0.001*	<0.001*	1.00
Intersections SCP	1096.65 ± 349.48	824.04 ± 288.95	726.04 ± 259.98	<0.001*	<0.001*	0.19
Intersections DCP	1945.96 ± 517.93	1233.63 ± 663.61	1042.35 ± 389.11	<0.001*	<0.001*	0.202
Mean vessel diameter SCP, μm	27.55 ± 0.16	27.3 ± 0.4	31.66 ± 32.27	1.00	1.00	0.831
Mean vessel diameter DCP, μm	27.26 ± 0.29	27.18 ± 0.35	27.22 ± 0.32	0.833	1.00	1.00
Fractal dimensions SCP	1.68 ± 0.02	1.67 ± 0.03	1.64 ± 0.003	0.020*	<0.001*	<0.001*
Fractal dimensions DCP	1.71 ± 0.02	1.69 ± 0.03	1.67 ± 0.03	<0.001*	<0.001*	<0.001*
Vessel density SCP, %	52.47 ± 3.44	47.59 ± 5.08	43.36 ± 3.58	<0.001*	<0.001*	<0.001*
Vessel density DCP, %	59.14 ± 2.78	54.29 ± 4.41	50.05 ± 3.73	<0.001*	<0.001*	<0.001*
Acircularity index	0.78 ± 0.12	0.70 ± 0.12	0.59 ± 0.14	0.024*	<0.001*	<0.001*

Groups were compared using 1-way analysis of variance (ANOVA) with post hoc Bonferroni correction. HbA1c: glycated hemoglobin, percent of total hemoglobin. IOL, intraocular lens.

* Bonferroni adjusted *P* value < 0.05 was considered statistically significant.

PDR. Furthermore, the same parameter was recently shown to be an important indicator of microvascular changes in early DR.^{28,29} Finally, acircularity index has been shown to be highly sensitive to early DR changes.¹⁴ Based on these previous studies, it is therefore not surprising that these parameters, in combination, could differentiate eyes with NoDR and any DR as well as eyes with NPDR and PDR. Our results as well as those from the majority of OCTA publications suggest that progression of DR differentially affects the SCP and DCP, and future studies are warranted to illuminate these specific effects. In a previous OCTA study, our group reported that adjusted flow index, an indirect measure of blood velocity,

decreased more rapidly in the DCP with increasing DR severity when compared to the SCP.^{11,30} More severe reduction in blood flow in the DCP provides a rationale for the ability of DCP vessel density to discriminate the stages of retinopathy in the current study.

Previous studies used a variety of OCTA segmentation algorithms, including full-thickness OCTA measurements,^{6,7} while others analyzed individual capillary plexus layers.^{25,26} Some of these studies, like the study by Durbin et al.,¹⁵ showed that SCP parameters had a higher diagnostic accuracy at differentiating different grades of diabetic retinopathy, while others identified DCP parameters as more important.^{3,28} These

TABLE 2. Multivariable Logistic Regression Model for Eyes With Nonproliferative Diabetic Retinopathy Versus Proliferative Diabetic Retinopathy

Parameter	Odds Ratio, OR	95% Wald Confidence Limits OR		<i>P</i> Value	<i>P</i> Value After GEE*	AUC, Sensitivity, and Specificity
Adjusting for age and sex, 110 eyes of 70 patients						
RecFAZ SCP	0.626	0.404	0.969	0.0358	0.7448	AUC = 0.845
Vessel density DCP	0.840	0.742	0.951	0.006	0.0991	Sensitivity = 0.86
Acircularity	0.003	<0.001	0.174	0.0045	0.4220	Specificity = 0.70
Males, adjusting for age, 63 eyes of 38 patients						
RecFAZ SCP	0.626	0.365	1.071	0.087	0.571	AUC = 0.819
Vessel density DCP	0.857	0.735	1.000	0.050	0.1898	Sensitivity = 0.83
Acircularity index	0.003	<0.001	0.695	0.036	0.4257	Specificity = 0.75
Females, adjusting for age, 47 eyes of 32 patients						
RecFAZ SCP	0.590	0.266	1.310	0.195	0.141	AUC = 0.889
Vessel density DCP	0.809	0.652	1.004	0.054	0.191	Sensitivity = 0.90
Acircularity index	0.006	<0.001	2.530	0.097	0.739	Specificity = 0.81

RecFAZ, reciprocal FAZ.

* GEE correction for correlation between both eyes without adjusting for age.

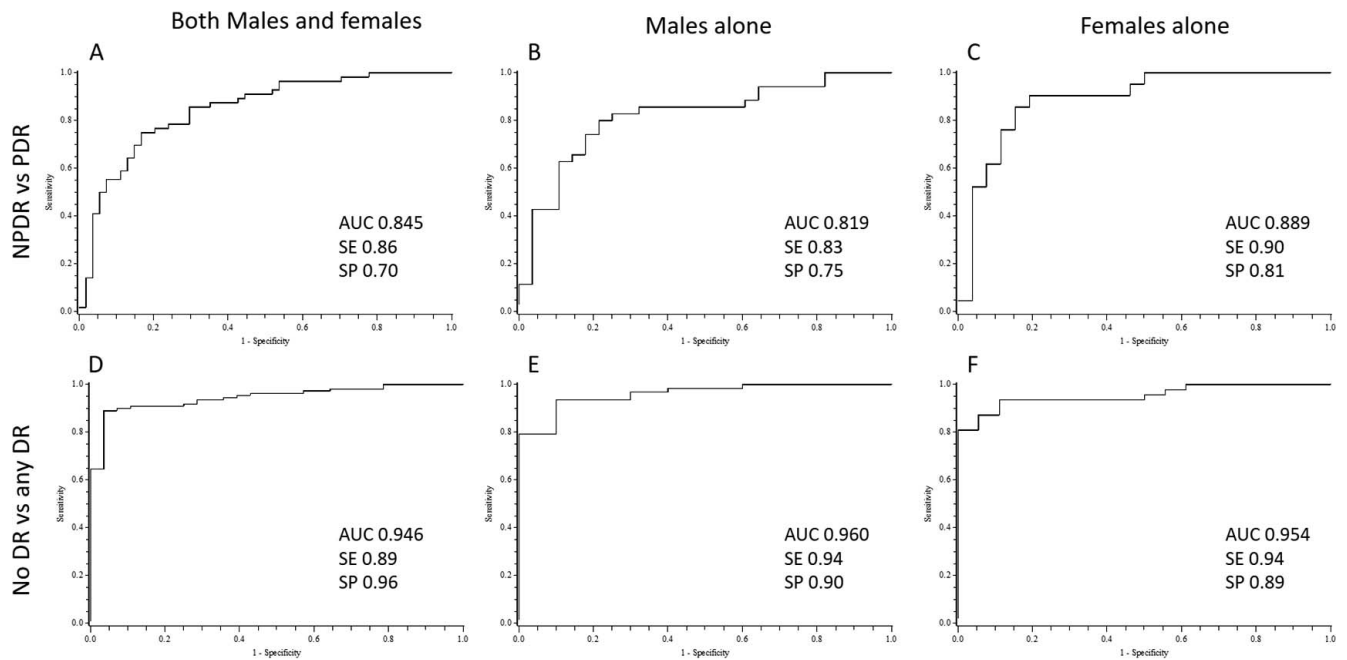


FIGURE. Receiver operating characteristic (ROC) curves for the combined parameter binary regression model. *Upper row* shows the ROC curves for eyes with nonproliferative diabetic retinopathy (NPDR) versus proliferative diabetic retinopathy (PDR). *Lower row* shows the ROC curve for eyes with no diabetic retinopathy (DR) versus those with any DR. SE, sensitivity; SP, specificity.

studies use highly variable segmentation schemes, with some devices using retinal sublayer boundaries while others use percentage of retinal thickness to segment the retinal capillary plexuses, which may confound the results of these studies.³¹ Our final model identified a combination of parameters from the SCP and DCP, highlighting the value of incorporating parameters from both capillary plexuses in differentiating early and late stages of DR. We have recently shown that SCP parameters are significantly altered in early DR (before clinical retinopathy) compared to healthy eyes.¹¹ In contrast, with increasing severity of DR, the deeper plexuses show more significant changes, compared to the SCP.^{11,30} This is further supported by a recent study that used graders to judge the presence or absence of nonperfusion in OCTA en face scans, and showed that the diagnostic efficacy increased when the individual capillary layers (SCP, MCP, and DCP) were evaluated, compared to the full-thickness angiograms.^{25,26}

Another aim of the study was to determine if the model works equally well for both sexes, as OCT and OCTA parameters are influenced by sex.^{30,32} While the model performed equally well in the NoDR versus any DR analysis (AUC 0.96 in males and 0.954 in females) (Table 4), we found that in the NPDR versus PDR group the model performed slightly better in females (AUC 0.889, sensitivity 90% and specificity 81%) compared to males (AUC 0.819, sensitivity 83% and specificity 75%; Table 2). While the source of these differences remains unclear, these results should be considered cautiously in light of the small sample size. Future studies using larger cohorts are necessary to explore these potential sex differences.

It is important to note that the parameters included in the model were deduced by applying the regression model to differentiate NPDR and PDR. We did not run a separate binary logistic regression model for NoDR and any DR. Using this approach the combined model achieved a sensitivity of 86% and a specificity of 70% in the NPDR versus PDR group, compared to the previously reported sensitivity/specificity of 90%/44% for the SCP vessel density alone and 91%/50% for the

DCP vessel density alone.³³ Furthermore, the same model performed well in the NoDR versus any DR group with a sensitivity of 89% and specificity of 96%, which compares favorably with previous attempts to differentiate normal eyes and eyes with DR, with the important difference that it is considerably harder to detect changes between NoDR and eyes with any DR.^{5,34}

Limitations of our study include the relatively small number of eyes, particularly in the NoDR group. Furthermore, our model did not have sufficient power to explore grades of NPDR, which could be an important area for future research.^{35,36} We relied on automatic segmentation to identify the SCP and DCP with the possibility of segmentation errors. Furthermore, we did not assess the effect of DME on the model, as most of our cases did not have center-involving macular edema. Future studies assessing this model in a larger cohort of patients, as well as including eyes with more severe DME, would be necessary for validating this technique for use in eyes with DME. Most PDR cases (57%) in the current study had previous PRP laser, which may have influenced the difference between eyes with NPDR and PDR.³⁷⁻³⁹ The effects of PRP and anti-VEGF on the OCTA parameters are important future studies. Another limitation was the use of both eyes of the same patient. Although we used GEE to adjust for the

TABLE 3. Multivariable Logistic Regression Model and Individual Parameter Sensitivity/Specificity for Eyes With Nonproliferative Versus Proliferative Diabetic Retinopathy

Parameters in the Receiver Operating Curve	AUC	Sensitivity	Specificity
Reciprocal FAZ SCP	0.725	0.89	0.46
Vessel density DCP	0.790	0.84	0.65
Acircularity index	0.729	0.88	0.52
Combined regression model, both males and females	0.845	0.86	0.70

TABLE 4. Multivariable Logistic Regression Model for Eyes With Versus Those Without Diabetic Retinopathy

Parameter	Odds Ratio, OR	95% Wald Confidence Limits OR		P Value	P Value After GEE*	AUC, Sensitivity, and Specificity
Adjusting for age and sex, 138 eyes of 87 subjects						
RecFAZ SCP	0.802	0.680	0.946	0.009	0.017	AUC = 0.946
Vessel density DCP	0.574	0.433	0.760	<0.001	<0.001	Sensitivity = 0.89
Acircularity	<0.001	<0.001	0.226	0.0234	0.057	Specificity = 0.96
Males, adjusting for age, 73 eyes of 44 patients						
RecFAZ SCP	0.776	0.555	1.085	0.139	0.003	AUC = 0.96
Vessel density DCP	0.557	0.355	0.874	0.011	0.028	Sensitivity = 0.94
Acircularity index	<0.001	<0.001	224.209	0.255	0.426	Specificity = 0.90
Females, adjusting for age, 65 eyes of 43 patients						
RecFAZ SCP	1.632	0.798	3.339	0.1796	0.861	AUC = 0.954
Vessel density DCP	0.539	0.343	0.849	0.0076	0.034	Sensitivity = 0.94
Acircularity index	<0.001	<0.001	0.431	0.040	0.504	Specificity = 0.89

RecFAZ, reciprocal FAZ.

* GEE correction for correlation between both eyes without adjusting for age.

correlation between eyes of the same subject, the correlation between the two eyes was high, which increased the standard error estimate of parameters and caused their nonsignificance in the NPDR versus PDR model despite a highly significant AUC curve (Tables 2, 4). We also did not correct for axial length, which could be a source of error in quantitative OCTA parameters.⁴⁰ We acknowledge that using different OCTA devices or different segmentation boundaries for the SCP and DCP could impact the results of this study, emphasizing the importance of reaching consensus in the field.³¹

In conclusion, we present a model that combines OCTA parameters from the SCP and DCP to achieve high sensitivity and specificity for differentiating eyes with PDR from those with NPDR as well as eyes with any DR from those with NoDR. This model works equally well for males and females in eyes of diabetic subjects with and without DR. However, the model seems to achieve a slightly higher specificity in female subjects when differentiating NPDR from PDR. Future studies involving larger cohorts are needed to validate this model and to explore the sex differences with advancing DR severity in greater detail. In addition, we believe that future larger studies are important to examine the ability of this model to correlate with severity within the NPDR group. Validation studies using a different dataset and larger cohorts will be important to facilitate future clinical applications of the presented model as a screening and referral tool in DR.

Acknowledgments

Supported by National Institutes of Health 1DP3DK108248 (AAF) and research instrument and software support by OptoVue, Inc., Fremont, California, United States. The funding agencies had no role in study design, data collection and analysis, decision to publish, or preparation of the manuscript.

Disclosure: **M. Ashraf**, None; **P.L. Nesper**, None; **L.M. Jampol**, None; **F. Yu**, None; **A.A. Fawzi**, None

References

- Jia Y, Tan O, Tokayer J, et al. Split-spectrum amplitude-decorrelation angiography with optical coherence tomography. *Opt Express*. 2012;20:4710–4725.
- Park JJ, Soetikno BT, Fawzi AA. Characterization of the middle capillary plexus using optical coherence tomography angiography in healthy and diabetic eyes. *Retina*. 2016;36:2039–2050.
- Tan CS, Lim LW, Chow VS, et al. Optical coherence tomography angiography evaluation of the parafoveal vasculature and its relationship with ocular factors. *Invest Ophthalmol Vis Sci*. 2016;57:OCT224–OCT234.
- Zahid S, Dolz-Marco R, Freund KB, et al. Fractal dimensional analysis of optical coherence tomography angiography in eyes with diabetic retinopathy. *Invest Ophthalmol Vis Sci*. 2016; 57:4940–4947.
- Bhanushali D, Anegondi N, Gadde SG, et al. Linking retinal microvasculature features with severity of diabetic retinopathy using optical coherence tomography angiography. *Invest Ophthalmol Vis Sci*. 2016;57:OCT519–OCT525.
- Schottenhamml J, Moulton EM, Ploner S, et al. An automatic, intercapillary area-based algorithm for quantifying diabetes-related capillary dropout using optical coherence tomography angiography. *PLoS One*. 2016;36:S93–S101.
- Salz DA, de Carlo TE, Adhi M, et al. Select features of diabetic retinopathy on swept-source optical coherence tomographic angiography compared with fluorescein angiography and normal eyes. *JAMA Ophthalmol*. 2016;134:644–650.
- Takase N, Nozaki M, Kato A, Ozeki H, Yoshida M, Ogura Y. Enlargement of foveal avascular zone in diabetic eyes evaluated by en face optical coherence tomography angiography. *Retina*. 2015;35:2377–2383.
- Samara WA, Shahlaee A, Adam MK, et al. Quantification of diabetic macular ischemia using optical coherence tomography angiography and its relationship with visual acuity. *Ophthalmology*. 2017;124:235–244.
- Kim AY, Chu Z, Shahidzadeh A, Wang RK, Puliafito CA, Kashani AH. Quantifying microvascular density and morphology in diabetic retinopathy using spectral-domain optical coherence tomography angiography. *Invest Ophthalmol Vis Sci*. 2016;57:OCT362–OCT370.
- Nesper PL, Roberts PK, Onishi AC, et al. Quantifying microvascular abnormalities with increasing severity of diabetic retinopathy using optical coherence tomography angiography. *Invest Ophthalmol Vis Sci*. 2017;58: BIO307–BIO315.
- Lee H, Lee M, Chung H, Kim HC. Quantification of retinal vessel tortuosity in diabetic retinopathy using optical coherence tomography angiography. *Retina*. 2017;38:976–985.
- Bhardwaj S, Tsui E, Zahid S, et al. Value of fractal analysis of optical coherence tomography angiography in various stages of diabetic retinopathy [published online ahead of print July 18, 2017]. *Retina*. doi:10.1097/IAE.0000000000001774.

14. Krawitz BD, Mo S, Geyman IS, et al. Acircularity index and axis ratio of the foveal avascular zone in diabetic eyes and healthy controls measured by optical coherence tomography angiography. *Vision Res.* 2017;139:177-186.
15. Durbin MK, An L, Shemonski ND, et al. Quantification of retinal microvascular density in optical coherence tomographic angiography images in diabetic retinopathy. *JAMA Ophthalmol.* 2017;135:370-376.
16. Mastropasqua R, Toto L, Mastropasqua A, et al. Foveal avascular zone area and parafoveal vessel density measurements in different stages of diabetic retinopathy by optical coherence tomography angiography. *Int J Ophthalmol.* 2017; 10:1545-1551.
17. Sandhu HS, Eladawi N, Elmogy M, et al. Automated diabetic retinopathy detection using optical coherence tomography angiography: a pilot study [published online ahead of print January 23, 2018]. *Br J Ophthalmol.* doi:10.1136/bjophthalmol-2017-311489.
18. Early Treatment Diabetic Retinopathy Group. Grading diabetic retinopathy from stereoscopic color fundus photographs—an extension of the modified Airlie House classification: ETDRS report number 10. *Ophthalmology.* 1991;98:786-806.
19. Wilkinson CP, Ferris FL III, Klein RE, et al. Proposed international clinical diabetic retinopathy and diabetic macular edema disease severity scales. *Ophthalmology.* 2003;110: 1677-1682.
20. Ferreira T, Rasband W. *ImageJ User Guide: IJ 1.46r.* Bethesda, MD: National Institutes of Health; 2012.
21. Samara WA, Say EA, Khoo CT, et al. Correlation of foveal avascular zone size with foveal morphology in normal eyes using optical coherence tomography angiography. *Retina.* 2015;35:2188-2195.
22. Tam J, Dhamdhare KP, Tiruveedhula P, et al. Disruption of the retinal parafoveal capillary network in type 2 diabetes before the onset of diabetic retinopathy. *Invest Ophthalmol Vis Sci.* 2011;52:9257-9266.
23. Garrity ST, Iafe NA, Phasukkijwatana N, Chen X, Sarraf D. Quantitative analysis of three distinct retinal capillary plexuses in healthy eyes using optical coherence tomography angiography. *Invest Ophthalmol Vis Sci.* 2017;58:5548-5555.
24. Hotaling NA, Bharti K, Kriel H, Simon CG Jr. DiameterJ: a validated open source nanofiber diameter measurement tool. *Biomaterials.* 2015;61:327-338.
25. Hwang TS, Gao SS, Liu L, et al. Automated quantification of capillary nonperfusion using optical coherence tomography angiography in diabetic retinopathy. *JAMA Ophthalmol.* 2016; 134:367-373.
26. Hwang TS, Zhang M, Bhavsar K, et al. Visualization of 3 distinct retinal plexuses by projection-resolved optical coherence tomography angiography in diabetic retinopathy. *JAMA Ophthalmol.* 2016;134:1411-1419.
27. Kim K, Kim ES, Yu SY. Optical coherence tomography angiography analysis of foveal microvascular changes and inner retinal layer thinning in patients with diabetes. *Br J Ophthalmol.* 2018;102:1226-1231.
28. Scarinci F, Picconi F, Giorno P, et al. Deep capillary plexus impairment in patients with type 1 diabetes mellitus with no signs of diabetic retinopathy revealed using optical coherence tomography angiography. *Acta Ophthalmol.* 2018;96:e264-e265.
29. Simonett JM, Scarinci F, Picconi F, et al. Early microvascular retinal changes in optical coherence tomography angiography in patients with type 1 diabetes mellitus. *Acta Ophthalmol.* 2017;95:e751-e755.
30. Onishi AC, Nesper PL, Roberts PK, et al. Importance of considering the middle capillary plexus on OCT angiography in diabetic retinopathy. *Invest Ophthalmol Vis Sci.* 2018;59: 2167-2176.
31. Fawzi AA. Consensus on optical coherence tomographic angiography nomenclature: do we need to develop and learn a new language? *JAMA Ophthalmol.* 2017;135:377-378.
32. Wang Q, Chan S, Yang JY, et al. Vascular density in retina and choriocapillaris as measured by optical coherence tomography angiography. *Am J Ophthalmol.* 2016;168:95-109.
33. Pedinielli A, Bonnin S, Sanharawi ME, et al. Three different optical coherence tomography angiography measurement methods for assessing capillary density changes in diabetic retinopathy. *Ophthalmic Surg Lasers Imaging Retina.* 2017; 48:378-384.
34. Chen Q, Ma Q, Wu C, et al. Macular vascular fractal dimension in the deep capillary layer as an early indicator of microvascular loss for retinopathy in type 2 diabetic patients. *Invest Ophthalmol Vis Sci.* 2017;58:3785-3794.
35. Boyer DS, Nguyen QD, Brown DM, Basu K, Ehrlich JS. Outcomes with as-needed ranibizumab after initial monthly therapy: long-term outcomes of the phase III RIDE and RISE Trials. *Ophthalmology.* 2015;122:2504-2513.
36. Brown DM, Schmidt-Erfurth U, Do DV, et al. Intravitreal aflibercept for diabetic macular edema: 100-week results from the VISTA and VIVID Studies. *Ophthalmology.* 2015;122: 2044-2052.
37. Mendrinos E, Mangioris G, Papadopoulou DN, Dosso AA, Pournaras CJ. Retinal vessel analyzer measurements of the effect of panretinal photocoagulation on the retinal arteriolar diameter in diabetic retinopathy. *Retina.* 2010;30:555-561.
38. Grunwald JE, Brucker AJ, Petrig BL, Riva CE. Retinal blood flow regulation and the clinical response to panretinal photocoagulation in proliferative diabetic retinopathy. *Ophthalmology.* 1989;96:1518-1522.
39. Fekete GT, Green GJ, Goger DG, McMeel JW. Laser Doppler measurements of the effect of panretinal photocoagulation on retinal blood flow. *Ophthalmology.* 1982;89:757-762.
40. Linderman R, Salmon AE, Strampe M, Russillo M, Khan J, Carroll J. Assessing the accuracy of foveal avascular zone measurements using optical coherence tomography angiography: segmentation and scaling. *Trans Vis Sci Tech.* 2017; 6(3):16.